Magnetoresistance of Thallium*

J. C. MILLIKEN† AND R. C. YOUNG
Institute for Atomic Research and Department of Physics, Iowa State University, Ames, Iowa
(Received 4 October 1965; revised manuscript received 7 March 1966)

This paper presents a study of the magnetoresistance of several single crystals of high-purity thallium in magnetic fields up to 100 kG at liquid-helium temperatures. The experimental results are interpreted in terms of Soven's relativistic orthogonalized-plane-wave model for the Fermi surface of thallium. At low fields the magnetoresistance is in better agreement with the model than was previous work, while no evidence is found for an open orbit parallel to [0001]. Detailed results up to 54 kG are consistent with the model if incomplete magnetic breakdown is assumed and high-field results show that breakdown is not complete below 100 kG.

I. INTRODUCTION

IT was originally suggested by Mackintosh *et al.*[1] that low-field magnetoresistance measurements[1,2] of single crystals of thallium were consistent with a Fermi surface topologically similar to the nearly-free-electron model. This explanation assumed that magnetic breakdown occurred between the third and fourth Brillouin zones of the model across the (0001) face of the zone. Studies of the de Haas–van Alphen[3] and magnetoacoustic effects[4] were also consistent with this model. Soven's[5] relativistic orthogonalized-plane-wave (OPW) calculation gave a Fermi surface topologically quite similar to the free-electron model and a maximum breakdown field of approximately 40 kG. Neither the experimental results nor the calculation were able to show unambiguously[6] that the [0001] connectivity of the 4th-zone surface of the free-electron model was actually present on the real Fermi surface, however, and no experimental estimate of the breakdown field existed. In this work measurements of the magnetoresistance of thallium have been made at various magnetic fields up to 100 kG, to resolve ambiguities between the magnetoresistance at low fields and the Fermi-surface models and to study the development of magnetic breakdown in thallium at high magnetic fields.

In the next section, the theory of magnetoresistance and of magnetic breakdown is briefly discussed and models of the Fermi surface of thallium are described. In Sec. III the experimental method is described, while the experimental results are presented in Sec. IV. Finally, these results are discussed in terms of Soven's model.

II. THEORY

Theory of Magnetoresistance and Magnetic Breakdown

In the limit when the product of the cyclotron frequency (ω_c) and the relaxation time (τ) of a conduction electron is large ($\omega_c\tau \gg 1$ for all closed orbits), the character of the transverse magnetoresistance depends on two general features of the Fermi surface; the open or closed character of the orbits and the balance (compensation) or unbalance (discompensation) between electron and hole carriers.[7] The behavior expected for all possible cases is summarized in Table I.

The open orbits possible on a multiply connected Fermi surface can be classified as follows: A one-dimensional periodic (type-A) open orbit can exist only when the magnetic field is perpendicular to a rational direction in the crystal lattice. Two-dimensional, generally aperiodic (type-B) open orbits occur for a range of field directions around an axis of high symmetry when it is possible to propagate open orbits in all directions in a plane perpendicular to the axis of symmetry. These are not periodic except when the direction of propagation coincides with a rational direction in the plane.

If the energy gap across a Brillouin-zone face is small, as when otherwise degenerate bands are split by spin-orbit coupling, magnetic breakdown can occur and the

TABLE I. Magnetic field dependence of the transverse magnetoresistance in the limit $\omega_c\tau \gg 1$ for all closed orbits. (The longitudinal magnetoresistance always saturates in high fields.)

Topology	Behavior of transverse magnetoresistance
closed orbits uncompensated	saturates
closed orbits compensated	H^2
open orbits in a direction in k space making an angle α with the current	$H^2\cos^2\alpha$
open orbits in several directions in k space	saturates

*Work was performed at the Ames Laboratory of the U. S. Atomic Energy Commission. Contribution No. 1792.
† Present address: IBM, Poughkeepsie, New York.
[1] A. R. Mackintosh, L. E. Spanel, and R. C. Young, Phys. Rev. Letters **10**, 434 (1963).
[2] N. E. Alekseevskii and Yu. P. Gaidukov, Zh. Eksperim. i Teor. Fiz. **43**, 2097 (1962) [English transl.: Soviet Phys.—JETP **16**, 1484 (1963)].
[3] M. G. Priestley, Bull. Am. Phys. Soc. **9**, 239 (1964).
[4] J. A. Rayne, Phys. Rev. **131**, 653 (1963).
[5] P. Soven, Phys. Rev. **137**, A1706 (1965).
[6] P. Soven, Phys. Rev. **137**, A1717 (1965).
[7] E. R. Fawcett, *Advances In Physics* (Francis & Taylor, Ltd. London, 1964), Vol. 13, p. 139.

electron has a finite probability P of tunneling through the gap, given by

$$P=\exp(-H_0/H), \tag{1}$$

where H is the magnetic field and H_0 is a characteristic breakdown field. For nearly free electrons with an energy gap Δ, and H in the z direction, Blount[8] gives

$$H_0=\pi\Delta^2/4\hbar e v_x v_y, \tag{2}$$

where v_x and v_y are components, parallel and perpendicular to the zone boundary, of the "free-electron velocity" at the zone boundary, i.e., the velocity which the electron would have in the absence of the energy gap. In the special case where $v_x=v_y$ and there is no component of v parallel to the field, Eq. (2) for H_0 reduces to

$$H_0=\pi\Delta^2 m/4\hbar e E_F, \tag{3}$$

where m is the electronic mass and E_F is the Fermi energy.

In the more general case where the field is still parallel to the zone face but the free-electron velocity at the relevant zone face makes an angle η with the face and its component parallel to the face makes an angle φ with the magnetic field, Eq. (3) must be multiplied by the factor

$$(\sin\varphi \sin 2\eta)^{-1}. \tag{4}$$

The effect of this correction is always to increase H_0 above its value in Eq. (3). If H is not parallel to the zone face, H_0 is further increased above the value given by Eq. (3). If the relation of the electron velocity to its energy involves an effective mass m^* which is different from the free-electron mass m, Eq. (3) must be multiplied by m^*/m.

If the nearly-free-electron description is not adequate, Chambers[9] has proposed the expression

$$H_0=\pi\hbar/2e[kg^3/(a+b)]^{1/2}, \tag{5}$$

where k_g is the separation of the two orbits in k space, while a^{-1} and b^{-1} are the radii of curvature of the respective orbits. This reduces to Eq. (2) for nearly free electrons.

Magnetic breakdown will affect the magnetoresistance if it causes a change in either of the two topological characteristics of the Fermi surface, open orbits or compensation. In general, it would be expected that the behavior of the magnetoresistance would reflect the topologies in the field ranges $H<H_0$, $H>H_0$, with a transitional range of behavior near H_0. Detailed specimen calculations by Falicov and Sievert[10] have shown that this prediction is modified in several ways. The transitional behavior is exhibited at a field H_m which is less than the field H_0, the typical relation being of the form

$$H_m=H_0/(A+B\tau), \tag{6}$$

where A and B are positive constants. Thus, they point out that changes in the character of the magnetoresistance are complete at fields below H_0 and that values of H_0 estimated from magnetoresistance results may therefore be low. If the topology after breakdown is one which causes the magnetoresistance to saturate, the value of the saturated resistance will be much higher than the usual values $\rho(H)/\rho(0)$ of order 1–10. This is because the random probability of the electron's following or leaving its breakdown orbit introduces an incoherent scattering process which shortens the relaxation time and so decreases the conductivity. Falicov and Sievert predict that the resistance at saturation will be proportional to ω_0 (assuming $\omega_0\tau\gg1$), where $\omega_0=eH_0/m$, but will be independent of τ.

Fermi-Surface Models for Thallium

Thallium is a hexagonal close-packed metal with a hexagonal reciprocal lattice. In the absence of spin-orbit coupling, the energy gap across the (0001) face (AHL in Fig. 1) between the third and fourth Brillouin zones would be zero. This degeneracy is lifted by the spin-orbit coupling except along the lines AL, the energy gap varying from zero on a line AL to a maximum value at a corner H.

The third and fourth zones of the free-electron model are shown in Fig. 1(a). The typical open orbit can propagate in a direction parallel to the (0001) plane if breakdown allows it to tunnel from the third to the fourth zones. Near the point K, the fourth-zone surface is extended in the [0001] direction and on the free-electron model is actually multiply connected in this direction, the connecting region being referred to as a "post." The fourth-zone surface also has a network of arms in the plane ΓMK, but Soven's[5] calculation suggests that they are actually much reduced in size, so

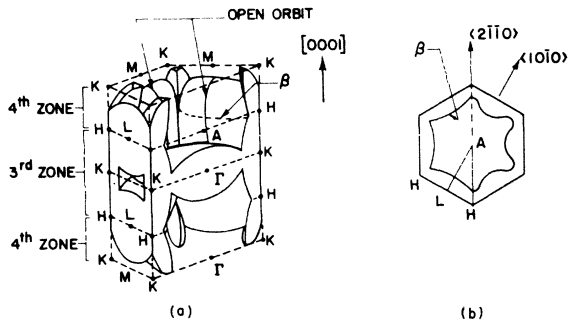

FIG. 1. (a) Third and fourth zones of the free-electron model for thallium. The typical open orbit is able to propagate parallel to a direction in the basal plane if breakdown allows it to cross the zone face AHL between the third and fourth zones. (b) A (0001) section of the fourth-zone surface on the plane AHL, showing the free-electron-model section on the left and the ROPW model section on the right.

[8] E. I. Blount, Phys. Rev. **126**, 1636 (1962).
[9] R. G. Chambers (to be published).
[10] L. M. Falicov and P. R. Sievert, Phys. Rev. **138**, A22 (1965).

they have been omitted from Fig. 1. Other small parts of the Fermi surface lie in the fifth and sixth zones.

Soven's[5] relativistic OPW calculation gives a Fermi surface (the ROPW model) which is topologically similar to the nearly-free-electron model. Using Eq. (3), Soven estimates the largest value of H_0 to be approximately 40 kG. This largest value of H_0 corresponds to the point where the Fermi surface intersects the line AH. The posts of the fourth zone of the nearly-free-electron surface are so reduced in size on the ROPW model that it is quite possible for them to be pinched off, so that the fourth-zone surface is possibly not multiply connected in the [0001] direction. Soven's calculation was not accurate enough to decide whether the posts were connected or not and Soven[6] showed that the published experimental work[1–4] was also inconclusive on this point.

III. EXPERIMENTAL TECHNIQUE

General

All the resistance measurements were made by the standard four-probe method. A battery and a bank of resistors provided a constant current in the range 10 mA to 1A, which was monitored by an ammeter. The voltage developed across the sample was amplified by a Keithley model 149 milimicrovoltmeter and displayed on the Y axis of an X-Y recorder. Most of the observations were taken by rotating the specimen about its axis in a constant magnetic field. Rotation was performed by a synchronous motor which also turned a Helipot. The voltage across the Helipot was displayed on the X axis of the recorder so that a plot of resistance versus angle of rotation of the magnetic field about the specimen axis was produced automatically. Measurements of resistance versus magnetic field were taken by automatically sweeping the field while a signal proportional to the field was fed to the X axis of the recorder.

Specimens

99.999% pure thallium, provided by the American Smelting and Refining Company and by the Cominco Inc. was used. It was not possible to prepare oriented single crystals by normal seeding techniques because thallium undergoes a crystallographic phase transition at 234°C, below its melting point. Therefore, two other techniques were used. Single crystals of arbitrary orientation were prepared from the ASR thallium by a strain-anneal technique. It was later found that the raw thallium provided by Cominco Inc. contained large crystallites from which suitable oriented single crystals were fabricated by spark cutting. The orientations of the specimens actually used are shown in Table II and also plotted on the stereogram of Fig. 6(b).

The resistivity ratio $\rho_{273°K}/\rho_{4.2°K}$ was in the range 3000–5000 for the stain-annealed specimens and 8000 for the Cominco specimens. Because the Debye Θ for thallium is only 100°K, phonon scattering is still appreciable at liquid-helium temperatures. Direct measurement of the residual resistance is not possible because thallium becomes superconducting at 2.38°K. Measurements showed that typically the resistance was halved in cooling from 4.2°K to just above the superconducting transition temperature. Spanel[11] measured the resistance of comparable specimens at 1°K in various magnetic fields above the superconducting critical field and, by extrapolating to zero field, found that the residual resistance was 2–3 times lower than the resistance at 4.2°K. The residual resistivity ratios $\rho_{273°K}/\rho_{1°K}$ are estimated to be in the range 10 000–25 000. Because it was not possible to measure $\rho(0)$ at 1°K directly, results will be presented in the form $\rho_T(H)/\rho(0)_{4.2°K}$ instead of the conventional $\rho_T(H)/\rho_T(0)$.

TABLE II. Specimens.

Specimen	$\rho_{273°K}/\rho_{4.2°K}$	Angle of specimen axis to [0001]	Angle of $(2\bar{1}\bar{1}0)$ plane to plane through specimen axis and [0001]
Tl-1[a]	5×10^3	71°	0°
Tl-2[a]	3×10^3	85°	12°
Tl-4[a]	5×10^3	0°	...
Tl-6[b]	8×10^3	0°	...
Tl-7[b]	8×10^3	26°	16°

[a] American Smelting and Refining Company.
[b] Cominco Inc.

The strain-annealed specimens were cylinders approximately 1.5 cm long and 0.1–0.2 cm in diameter, prepared by extruding polycrystalline thallium through a circular die and then annealing. The Cominco specimens were spark-cut parallelepipeds of about the same size. All were crystallographically oriented by back reflection x-ray photographs. To allow a specimen to be interchanged between several specimen holders without damage, it was mounted in the Teflon boat shown in Fig. 2. Four copper leads were soldered to the specimen using low melting point solder, the current leads being soldered at the ends and the potential leads at about 0.2 cm from the ends. The leads were threaded through

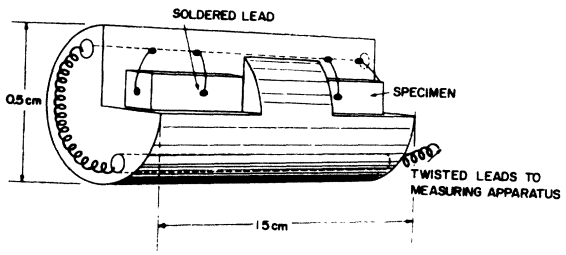

FIG. 2. Specimen boat.

[11] L. E. Spanel, Ph.D. thesis, Iowa State University of Science and Technology, Ames, Iowa, 1964 (unpublished), p. 52.

the boat as shown in Fig. 2 and twisted together so that the boat could be rotated without damaging the specimen or inducing pickup voltages in the leads. The specimen was lightly secured in the holder by Duco cement.

Magnets and Specimen Holders

Measurements were made up to about 28 kG using a conventional electromagnet, up to 55 kG using a superconducting solenoid, and a few measurements up to 100 kG using a conventional copper solenoid at the National Magnet Laboratory. Because a different specimen holder was used for each magnet, each will be described separately.

The measurements up to 28 kG were made in a Magnion, UF 10-5, electromagnet using a conventional metal Dewar system in which temperatures below 4.2°K were reached by pumping on the liquid helium. The specimen holder is shown in Fig. 3(a). The specimen was mounted horizontally and rotated about its axis while the angle θ between the specimen axis and the magnegic-field direction could be varied by rotating the electromagnet on its base. Since the transverse magnetoresistance was much larger than the longitudinal magnetoresistance for all the measurements taken, the anisotropy of the resistance for θ values other than 90° was interpreted as reflecting only the transverse magnetoresistance.

The Magnion superconducting solenoid was able to reach a field of 55 kG. The bore of the solenoid was 1 in. in a 4.2°K environment. In order to work at the lower temperatures at which the resistivity of pure thallium is residual, it was necessary to insert an inner Dewar system (Fig. 4) in which the temperature could be reduced by pumping to approximately 1°K while the solenoid remained at 4.2°K. The Dewar was filled with liquid helium by condensing helium gas; the 20 cc of liquid it contained lasting typically for 4 h at 1°K when a current of 300 mA was passing through the specimen. The boat was inserted into the center of a Teflon pulley wheel which was rotated about a horizontal axis by a stainless-steel wire.

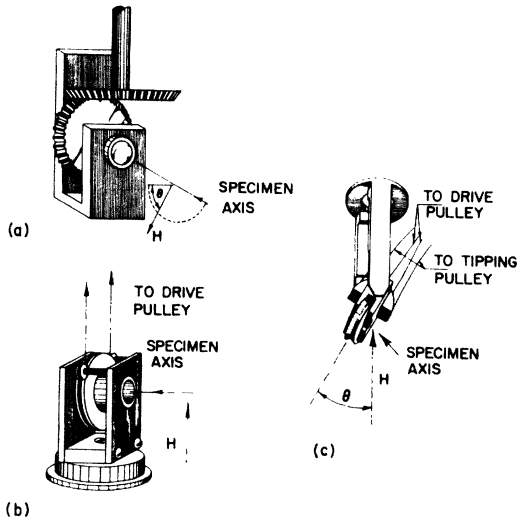

FIG. 3. Specimen holders: (a) for electromagnet, (b) for superconducting solenoid, and (c) for high-field studies. In each case the specimen boat was inserted where "specimen axis" is indicated.

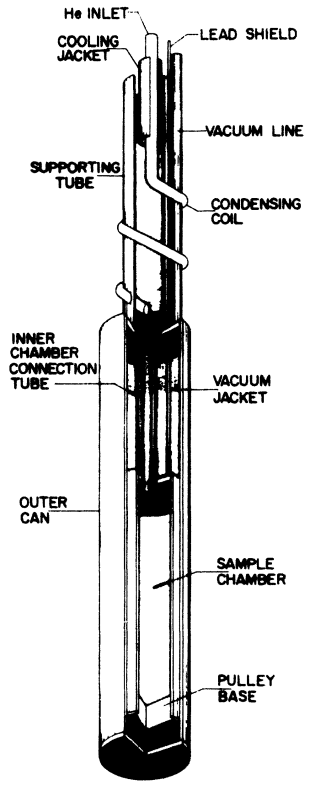

FIG. 4. Inner Dewar system for superconducting solenoid.

A more versatile specimen holder [Fig. 3(c)] was used for the high-field measurements at the National Magnet Laboratory. The specimen was rotated about its axis by stainless-steel wires while the axis of the specimen could also be tipped by two more stainless-steel wires; thus, it was possible for the field to sweep latitude lines about the specimen axis while using a solenoid. This specimen holder was used with a conventional metal Dewar system, the temperature being reduced below 4.2°K in the normal way by pumping.

Some care was required to eliminate errors due to the backlash in the rotating devices. The symmetry of the results was used both to calibrate the rotation and to determine the setting for which the magnetic field was perpendicular to the specimen axis.

IV. EXPERIMENTAL RESULTS

Low-Field Results

Figure 5 shows a typical rotation diagram for Tl-1 at 27 kG and 1°K. This is generally similar to the results of Alekseevskii and Gaidukov,[2] the resistance at 90°

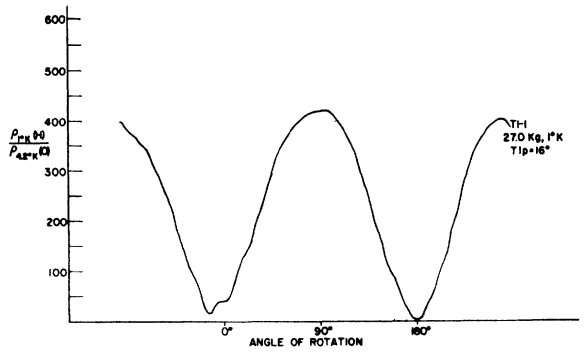

FIG. 5. Typical rotation diagram of resistivity versus angle of rotation about specimen axis for Tl-1, 180° of rotation being at the nearest approach of the field to the [0001] axis. This diagram is asymmetric because the magnetic field made an angle of less than 90° to the specimen axis.

varying approximately as H^2. This diagram is not symmetric about 90° because the magnetic field was set at an angle θ of 74° to the specimen axis. At 180° rotation, the magnetic field was approximately 3° from the c axis while at 0° it was 35° from the c axis. While the resistance near 0° exhibited approximately the $H^2\cos^2\alpha$ variation typical of aperiodic (type-B) open orbits, an extra dip which appears to be due to a periodic (type-A) open orbit can be seen near 0°. The boundary between type-A and type-B open orbits for the purer specimen Tl-7 is shown in Fig. 6(a). The region of type-B open orbits gives way to type-A open orbits at about 24° from the c axis and while type-A orbits persist all the way to the basal plane when the magnetic field is perpendicular to the $\langle 10\bar{1}0\rangle$ and $\langle 2\bar{1}\bar{1}0\rangle$ directions, a "whisker" of type-A orbits at an intermediate angle persists only to 38°. The field directions for these orbits are shown on the stereogram of Fig. 6(b). This structure was not reported by Alekseevskii and Gaidukov who worked only

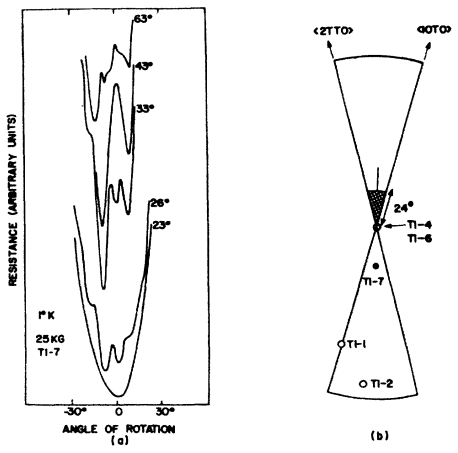

FIG. 6. (a) Rotation diagrams for Tl-7, indexed by the angle of closest approach of the field to the [0001] axis. (b) Stereogram showing specimen axes on the lower half and magnetic field directions for which open orbits were observed for Tl-7 on the upper half.

at 22 kG and 4.2°K but has been resolved in our work because of the increase of τ, resulting both from a higher purity specimen and lower temperatures.

Both for Tl-1 and Tl-2, that part of the rotation diagram near 90° was carefully examined for evidence of an open orbit along [0001]. When the field is perpendicular to this direction, the open orbit should manifest itself by a change in the behavior of the resistivity from AH^2 for a compensated metal to $BH^2\cos^2\alpha$ for an open orbit whose direction in reciprocal space makes an angle α to the specimen axis, A and B being approximately constant coefficients. For Tl-1 and Tl-2 the angle α had values of 71° and 85°, giving quite small $\cos^2\alpha$ values of 0.11 and 0.008, so that a minimum would be expected in the resistance anisotropy when the field was perpendicular to [0001]. No minimum was

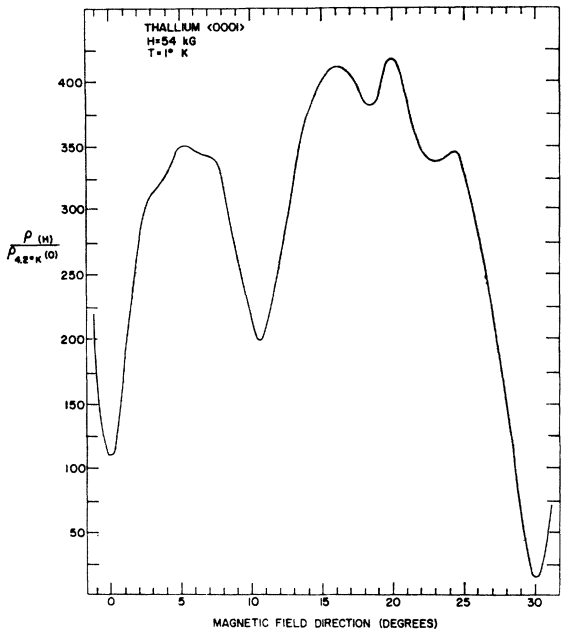

FIG. 7. Rotation diagram for [0001] specimen Tl-4 at 1°K and 54 kG. The magnetic field was perpendicular to the specimen axis.

observed over the field range from 5 to 20 kG, either at 4.2°K or at lower temperatures. It is possible that $B\approx A\cos^2\alpha$ for one of our values of α but the values of $\cos^2\alpha$ are in too great a ratio (14:1) for this to obscure the effect for both specimens.

As a further check, the rotations were also performed with the field tipped at angles to the specimen such that it was simultaneously perpendicular both to [0001] and to one of the directions, $\langle 10\bar{1}0\rangle$ or $\langle 2\bar{1}\bar{1}0\rangle$, for which open orbits exist in the basal plane even at low fields. The expected minimum, reflecting the saturation caused by two open orbits in different directions, was not observed. In summary, no evidence was found for an open orbit along [0001].

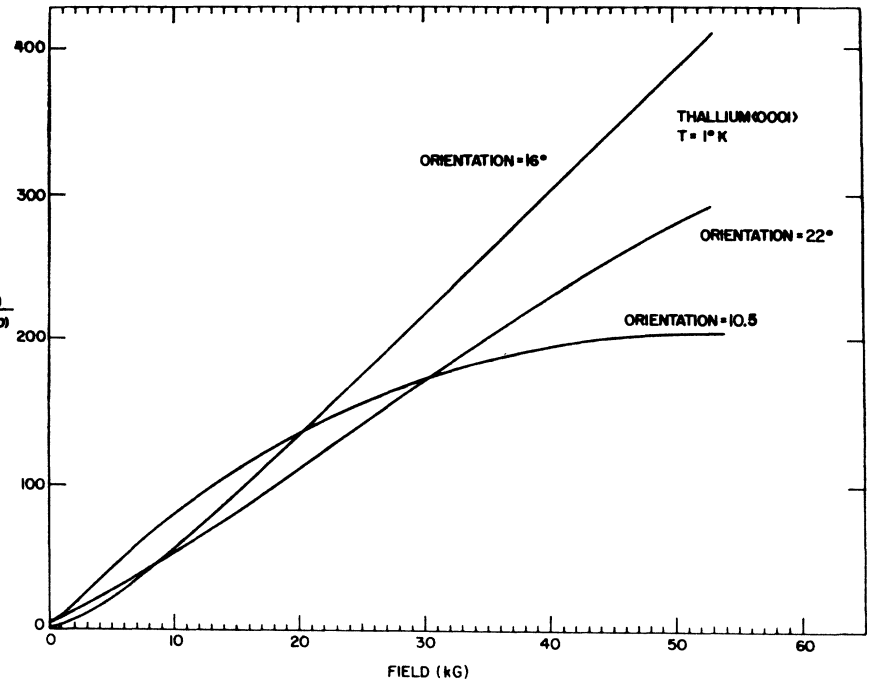

FIG. 8. Field dependences for Tl-4 at 1°K. The orientations correspond to the rotation readings of Fig. 7.

Results up to 54 kG

The previous measurements[1,2] of the transverse magnetoresistance of a c-axis specimen at fields up to 31 kG at 1°K and 22 kG at 4.2°K were extended up to 54 kG both at 4.2°K and at 1°K. Figure 7 shows a rotation diagram for the c-axis specimen at 54 kG and 1°K. The field dependence at several field orientations is shown in Fig. 8. Here, 16° corresponds to a maximum on the rotation diagram while 10.5° and 22° are approximately at minima.

The minima observed are summarized in Table III and are compared with those reported by Alekseevskii and Gaidukov at lower fields. Several developments compared to lower fields should be noted. The field dependence at 16° is approximately linear between 25 and 54 kG, whereas the lower field results indicated that the linear region would lead to saturation by about 40 kG. Our work has shown that rather than saturating for all field directions, the resistance varies approximately linearly with magnetic field, not only for the maxima but also for some of the minima. The minimum at 23° was barely apparent at 31 kG, and was not mentioned by Alekseevskii and Gaidukov, but by 54 kG the resistance is saturating. This is in marked contrast to the minimum at 18.5° which was well resolved at 31 kG, but shows no tendency to saturation by 54 kG.

TABLE III. Field directions in which minima were observed in the anisotropy of the resistance of a c-axis specimen at 54 kG and 1°K.

Angle observed in this work[a]	Field dependence	Angle observed by Alekseevskii and Gaidukov at 30 kG
0°	saturated	0°
30°	saturated	30°
10.5°	saturated	11.5°
23°	saturating	not observed
18.5°	linear	18.5°
4.5°	linear	4.5°
7°	linear	not observed

[a] Angle of the field to $\langle 10\bar{1}0 \rangle$, corresponding to the angle of rotation in Figs. 7–10.

Figure 9 shows rotations for the c-axis specimen at 4.2°K. These rotations exhibit fewer minima. One noteworthy feature is the shift of a minimum from 8° at 21.6 kG to 10° by 54 kG. At 1°K this shift is complete by 30 kG so it appears to depend on the relaxation time of the electrons. The field dependence at 4.2°K was approximately linear for all field directions except for the minima at 0° and 30° which exhibited saturation.

Results at Very High Fields

Two runs at fields up to 100 kG were made at the National Magnet Laboratory. Rotation diagrams for the c-axis specimen Tl-6 are shown in Fig. 10(a). In spite of the relatively high noise level and lower resolution, several useful observations can be made. The minimum at 23° is very well developed at 1.5°K and 90 kG while even at 4.2°K it is better developed at 90 kG than is the minimum at 18.5°. The maximum at 16° in the 54 kG work is less dominant at 90 kG and 4.2°K while at 90 kG and 1.5°K it appears to be changing into a minimum. The magnetic field dependence for Tl-6, Fig. 10(b), shows that even at 4.2°K, the resistance at

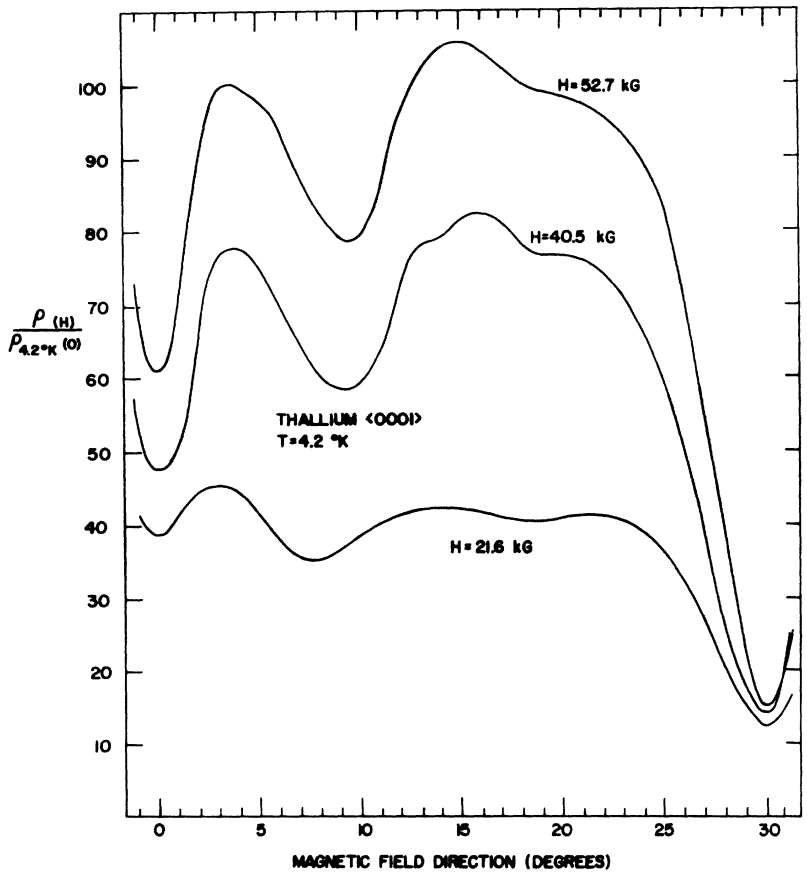

FIG. 9. Rotation diagrams for Tl-4 at 4.2°K for several fields.

5° is changing from linear towards saturation by 100 kG, although at 19° it has still hardly started to saturate.

The magnetic field dependence for Tl-1 [also Fig. 10(b)] shows that above 80 kG the resistance of this specimen is falling away from its lower field dependence of $H^{1.8}$. It was not possible in the limited time available to make a complete examination of this feature although further work is desirable to establish its reliability and study further its development at even higher fields.

V. DISCUSSION

When magnetic breakdown is complete, the ROPW model predicts that the resistance of a c-axis specimen will saturate for all magnetic field directions in the basal plane, regardless of the connectivity of the posts in the 4th zone. If the posts are not connected in the [0001] direction, open orbits are possible in all directions in the basal plane, giving rise to saturation of the magnetoresistance because α in the formula $H^2\cos^2\alpha$ of Table I is 90°. Breakdown changes thallium from compensated to uncompensated so that saturation would still occur even if the posts were connected and happened to cause all the orbits to close for some field directions. At 54 kG and 1°K the resistance has saturated for only a few field directions so breakdown is obviously not complete by this field. The high-field results suggest that only at fields of the order of 100 kG is the resistance beginning to saturate for all field directions. In view of the predictions of Falicov and Sievert[10] that the change in magnetoresistance is usually complete at fields below H_0, it is apparent that the maximum value of H_0 on the Fermi surface is unlikely to be less than 100 kG.

This maximum value of H_0 is considerably larger than the 40 kG predicted for the ROPW model using Eq. (3). This is not surprising, even assuming that the nearly-free-electron expressions for H_0 can be applied to the ROPW model, because the angle factor, Eq. (4), can only increase H_0. Later in the discussion, we will show the importance of this factor in thallium. An increase of the effective mass through the electron-phonon interaction will also increase H_0.

In the light of these large values for H_0, we will now discuss the low-field results. No experimental evidence was found for a [0001] open orbit at low fields. Such an orbit is possible on the fourth-zone surface if the posts are connected, though it will become closed if breakdown to the third zone occurs near H in the plane AHL. But this is the point at which the energy gap is largest so that at 10–20 kG the probability P of breakdown is negligible ($\sim e^{-5}$ to e^{-10}). Since no open

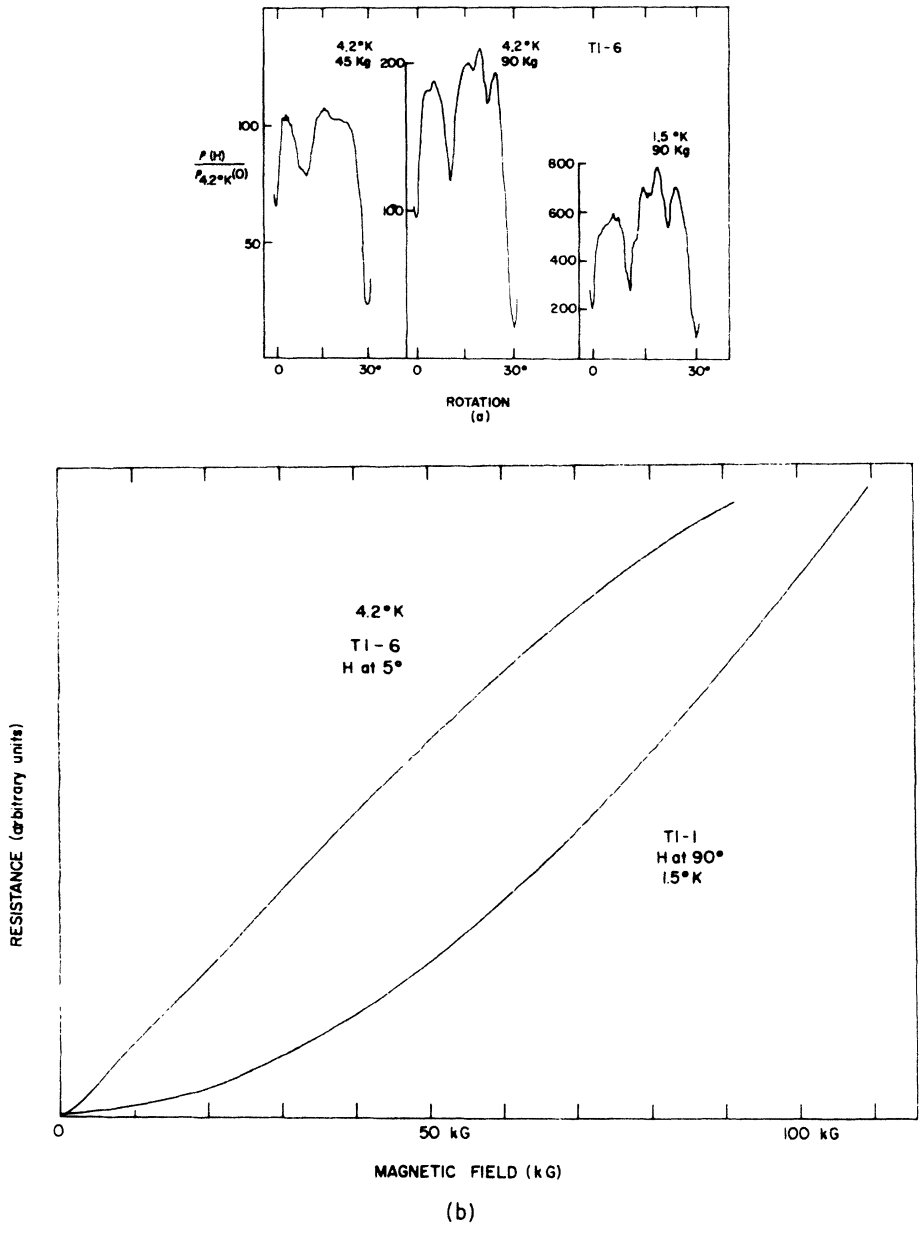

FIG. 10 (a) Rotations for Tl-6, (b) field dependences. Both taken at the National Magnet Laboratory.

orbits are observed, we conclude that the posts of the fourth-zone surface are not connected.

The stereogram of Fig. 6 indicates that at low fields a region of aperiodic (type-B) open orbits exists for magnetic field directions within about 24° of the c axis. This is in agreement with the ROPW model without breakdown, this angle being determined by the range of existence of the orbit β on the fourth-zone surface in Fig. 1. From their work at 4.2°K, Alekseevskii and Gaidukov[2] found that the region of type-B orbits existed for field directions up to 45° from the c axis. Soven had suggested that the discrepancy between the results of Alekseevskii and Gaidukov at 4.2°K and the model could be due either to a low τ or to breakdown. Our work with a purer specimen at 1°K shows that the discrepancy was in fact due to too low a τ to allow the structure in the magnetoresistance to be resolved. At 20 kG breakdown is far from complete for most field directions in the basal plane and is therefore even less developed for field directions at angles of 50°–60° to the basal plane.

We now turn to a more detailed consideration of the transverse magnetoresistance of the c-axis specimen. As noted in Table III, saturation was observed by 54 kG for several field directions and we will compare the behavior of the resistance for the three directions which saturate with large values, with the general features predicted by Falicov and Sievert[10] from their computa-

TABLE IV. Resistance of c-axis specimens at the minima which saturate at high value, compared to the fields at which saturation sets in.

Angle of field to $\langle 10\bar{1}0\rangle$ (deg)	$\rho(54\text{ kG})/1°\text{K}$ / $\rho(0)$[a] 4.2°K	Field at which[a] saturation sets in	$\rho(90\text{ kG})/1°\text{K}$ / $\rho(90\text{ kG})$[b] 4.2°K
0	120	~10 kG	2.1
10.5	200	~30 kG	2.4
23	350–400	50–60 kG	3.1

[a] Specimen Tl-4.
[b] Specimen Tl-6.

tions on a topologically similar model. In Table IV the saturation values of $\rho(H)$ for these directions are tabulated at 1°K. Falicov and Sievert predict that these values should be proportional to the appropriate values of H_0 and hence to field values at which the magnetoresistance shows saturation. From the data we have made a rough estimate of these fields for each direction and they are also listed in Table IV. It can be seen that they are approximately proportional to the values of $\rho(H)$.

The saturations at 10.5° and 23° for the c-axis specimen at 54 kG and 1°K were not observed at 4.2°K and the same field. This agrees with the predictions of Falicov and Sievert[10] that the saturation field should increase as τ decreases [Eq. (6)]. On the other hand, Falicov and Sievert also predict that the saturated value of ρ should be independent of τ and our results at 90 kG do not bear this out. At this field ρ saturates for several directions both at 4.2°K and 1°K but as shown in Table IV, the ratio of the resistivities is not unity but approximately 2–3.

We will now discuss the field directions for which saturation occurs for the c-axis specimens. We recall that open orbits in the basal plane lead to saturation of the magnetoresistance because the angle α in the formula $H^2\cos^2\alpha$ is 90°. For an open orbit to propagate in the basal plane, breakdown between the third- and fourth-zone surfaces must occur each time the orbit crosses the plane AHL. The energy gap Δ across the zone face varies from zero on the line AL to a maximum value on the line AH and this will be reflected in the breakdown field H_0. An open orbit propagating in an irrational direction in the basal plane will eventually pass through all points of intersection of the Fermi surface with the plane AHL and so will be forced to break through, at least occasionally, at points of largest H_0. But if the direction of propagation is parallel to a low-order rational direction, some orbits will be able to avoid the points of largest H_0 and so we expect that saturation will occur at lower fields. For example, the very low field saturation at 30° is due to open orbits propagating in the $\langle 10\bar{1}0\rangle$ direction, parallel to the line AL. The orbit which intersects AHL on AL encounters an energy gap of zero and nearby orbits break through only a very small gap, leading to saturation at very low fields.

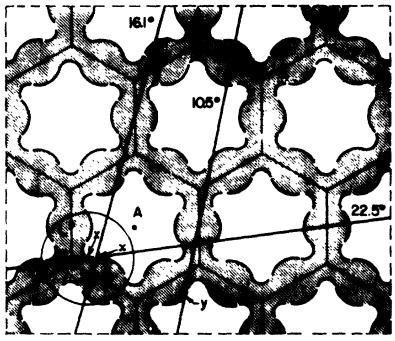

(a)

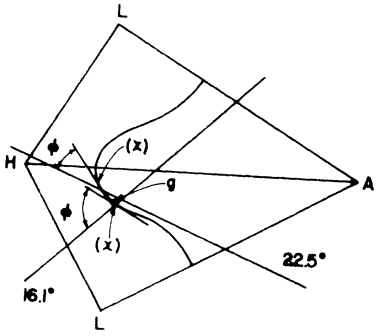

(b)

FIG. 11. (a) The fourth zone of the ROPW model on the plane AHL. The points of largest energy gap on the open orbits at 16.1°, 10.5°, and 22.5° are indicated as x, y, and z. (b) An enlargement of part of this surface showing that the open orbit at 22.5° breaks through at a point (z) nearer to the line AH, i.e., at a point of larger energy gap than the gap (x) broken through by the orbit at 16.1°. The angles φ are marked for these two orbits. For convenience we show φ here as the angle between the surface tangent (perpendicular to **v**) and the orbit direction (perpendicular to **H**).

Table V lists the low-order rational directions in the basal plane in reciprocal space, in order of shortest repeat distance. It can be seen that the observed features coincide well with the low-order rational directions. The first three directions show saturation as expected but the next saturation occurs for the quite high-order direction $\langle 13,\bar{5},\bar{8},0\rangle$ while no saturation is observed for six directions of lower order, and in particular at 54 kG and 1°K there is not even a minimum for the

TABLE V. Rational directions in the basal plane compared to the minima in the anisotropy of resistance of a c-axis specimen at 54 kG and 1°K.

Rational direction in reciprocal space	Angle of rational direction to $\langle 10\bar{1}0\rangle$	Position of observed minima	Field dependence
$\langle 2\bar{1}\bar{1}0\rangle$	30°	30°	Saturated
$\langle 10\bar{1}0\rangle$	0°	0°	Saturated
$\langle 5\bar{1}\bar{4}0\rangle$	10.9°	10.5°	Saturated
$\langle 7\bar{2}\bar{5}0\rangle$	16.1°	Not observed	···
$\langle 8\bar{1}\bar{7}0\rangle$	6.6°	7°	Linear
$\langle 3\bar{1}\bar{2}0\rangle$	19.1°	18.5°	Linear
$\langle 11\,\bar{4}\,\bar{7}\,0\rangle$	21.1°	Not observed	···
$\langle 11\,\bar{1}\,\bar{1}0\,0\rangle$	4.7°	4.5°	Linear
$\langle 4\bar{1}\bar{3}0\rangle$	13.9°	Not observed	···
$\langle 13\,\bar{5}\,\bar{8}\,0\rangle$	22.5°	23°	Saturating

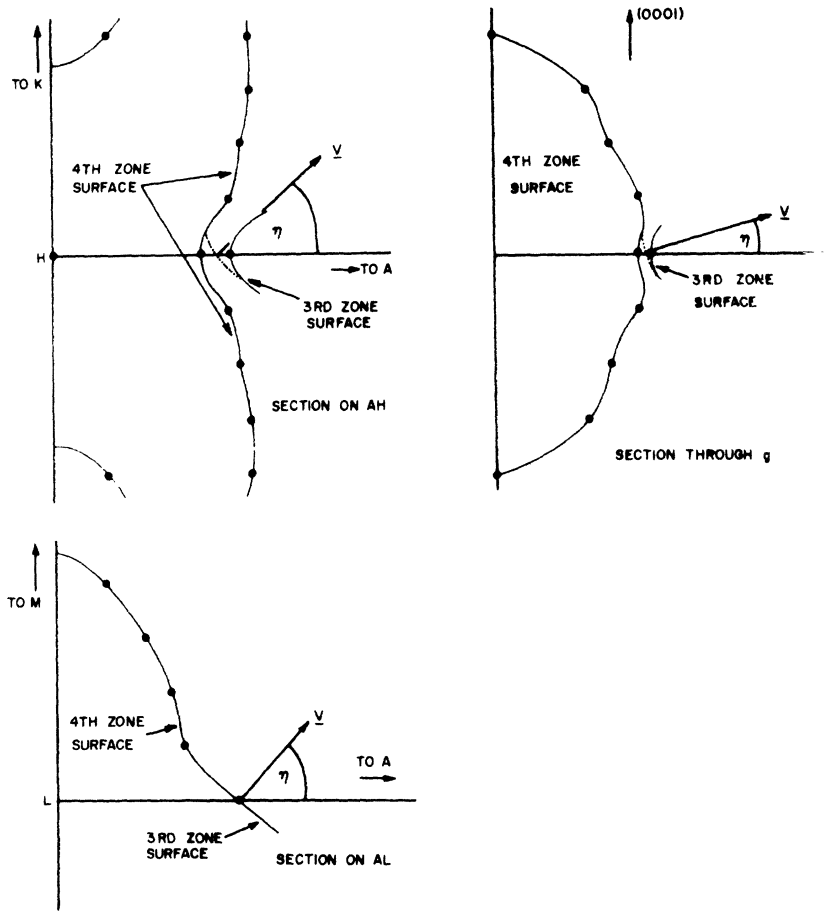

FIG. 12. Sections, perpendicular to the plane AHL, of the ROPW model in the region where breakdown connects the third- and fourth-zone surfaces. The sections are on the line AL, on the line AH, and through the point g, which is marked on Fig. 11(b). The dotted lines mark the "free-electron" interpolation and the angle η is indicated for each of the three sections.

$\langle 7,\bar{2},\bar{5},0\rangle$ direction of 16.1°. This suggests that an open orbit propagating parallel to the $\langle 13,\bar{5},\bar{8},0\rangle$ direction passes through points of smaller H_0 than does an orbit along $\langle 7,\bar{2},\bar{5},0\rangle$. This feature should presumably be apparent on the ROPW model.

In Fig. 11(a), a section of the fourth zone of the ROPW model in the plane AHL, we show the "optimum orbits" for the 10.5° and 22.5° directions for which saturation has set in by 54 kG as well as for the 16.1° direction which does not exhibit saturation, the optimum orbit being the orbit which stays as far as possible from those points of breakdown (near the line AH) where the energy gap is largest. The higher order directions take many reciprocal lattices to repeat and so we show only that part of a path which passes through the points of greatest energy gap encountered by the path. It can be seen that, as expected from the experimental observations, the largest energy gap crossed by the orbit at 10.5° [at y in Fig. 11(a)] is smaller than the largest energy gap crossed by the orbit at 16.1° [x in Fig. 11(a)]. However, it appears that the orbit at 22.5° crosses through a still larger energy gap [z in Fig. 11(a)] so that saturation should occur at a lower field for the 16.1° direction than for the 22.5° direction. Because this is not in agreement with the experimental results, the dependence of H_0 on the magnitude of the energy gap is not by itself a sufficient explanation.

Besides the energy gap, H_0 depends [Eq. (5)] on the angles φ and η which we now redefine in relation to the special case of the c-axis specimen of thallium. η is the angle between the "free-electron velocity vector" and the plane AHL while φ is the angle between the magnetic field (which is parallel to the plane AHL) and the component of velocity in the plane AHL. In Fig. 11(b) we have indicated φ for the paths at 16.1° and 22.5° and it can be seen that they both differ from 90° giving factors $1/\sin\varphi$ of 1.13 and 1.84.

Some values of η are illustrated in Fig. 12 where we show several sections, perpendicular to the plane AHL, of the third- and fourth-zone surfaces on the ROPW model near points of breakdown. Soven[5] gives contours of the fourth-zone surface for several k_z values and a contour of the third-zone surface on the plane AHL. By taking points from these contours we have constructed the fourth-zone sections and have drawn in possible third-zone sections which are compatible with the shape of the fourth-zone surface and intersect AHL in the correct position. We have dotted in the "free-electron path" which appears to be a reasonable interpolation and indicated the angle η. For the sections

on AH and AL, η is not far from the optimum of 45° but at g [marked in Fig. 11(b)] η is only about 15° so that the term $1/\sin 2\eta$ can introduce a correction factor of approximately two to H_0.

We see that the effect of the angles η and φ is considerable so that H_0 will not reflect simply the energy gap and our optimum orbits of Fig. 11(a) will not be the optimum orbits with respect to H_0. For example, shifting an orbit so that it passes through a point of larger energy gap may be more than compensated by the angle φ coming closer to 90°, and our discussion of η suggests the possibility of a lower H_0 at g than on the line AH in spite of the larger energy gap. H_0 depends in such a complicated way on the details of the ROPW model that any extension of our simple "optimum orbit" analysis is difficult. It is apparent, however, that consideration of the angle factor is essential. Detailed agreement with the experimental results could possibly be obtained by extending the calculations of Falicov and Sievert[10] to the more complicated case of thallium, suitable values of H_0 being calculated from the ROPW model.

We remarked earlier that the discrepancy between our experimental observation that breakdown was not complete below 100 kG and the 40 kG estimated by Soven was due to Soven's neglect of the dependence of H_0 on the angles. Since η and φ can each contribute a factor of 2 to H_0, we have shown that the angle term readily accounts for the discrepancy so that our results are not, in fact, in disagreement with the ROPW model.

Our discussion has so far assumed that the "nearly-free-electron" treatment was adequate and if this is not so, we should use Chambers' expression [Eq. (6)].[9] An examination of two of the sections of Fig. 12, those on the line AH and through g, show that in both sections the third- and fourth-zone orbits curve in the same direction when they intersect AHL. Chambers interprets a situation like this by subtracting $|a|$ from $|b|$, where a^{-1} and b^{-1} are the radii of curvature in the fourth and third zones, respectively. Thus for breakdown at any point between g and the line AH, H_0 is proportional to $(|b|-|a|)^{-1}$. Soven gives no contours of the third zone so it is impossible to estimate the radii of curvature of orbits on the third-zone surface. We remark, however, that unless the radii of curvature in the two zones are very different, H_0 will be large, as we have found experimentally.

We make no attempt to account for the detailed anisotropy for field directions and field values for which breakdown is not complete, such as the shift of minima with field observed at 4.2°K in fields up to 54 kG, since under these conditions account must be taken of the extended orbits which are produced by incomplete breakdown and for which $\omega_c\tau$ may be only of the order of unity.

The behavior of the resistance of Tl-1 at high fields, changing from variation as $H^{1.8}$ towards linear at fields above 80 kG, could reflect the possibility that the posts of the fourth-zone surface become connected by breakdown at high fields. This point requires detailed investigation at fields greater than 100 kG.

VI. CONCLUSIONS

Studies of magnetoresistance of thallium have shown that (1) the low-field magnetoresistance is now in good agreement with the predictions of the ROPW model. (2) The "posts" on the fourth zone of the ROPW model are not connected at low fields. (3) Breakdown across the hexagonal zone face between the third and fourth Brillouin zones is not complete below 100 kG. (4) The detailed behavior of the magnetoresistance of a c-axis specimen is not consistent with the ROPW model with magnetic breakdown, unless account is taken of the dependence of the breakdown probability on the angular relation of the electron velocity vector to the zone boundary, as well as the magnitude of the energy gap between the third and fourth zones.

ACKNOWLEDGMENTS

The use of the facilities of the National Magnet Laboratory and the willing cooperation of its staff are gratefully acknowledged. The specimens were prepared by J. F. Martin who also gave valuable assistance with the experimental equipment. We have benefited from discussions with Professor R. G. Chambers and Dr. A. R. Mackintosh.

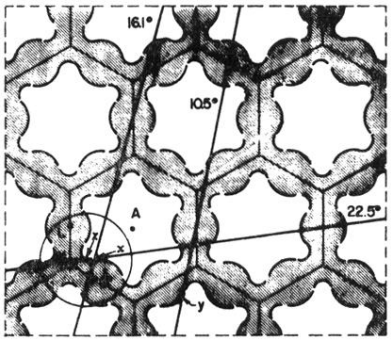

(a)

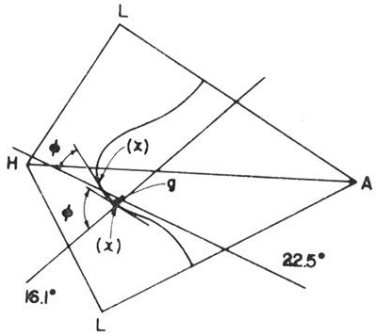

(b)

FIG. 11. (a) The fourth zone of the ROPW model on the plane AHL. The points of largest energy gap on the open orbits at 16.1°, 10.5°, and 22.5° are indicated as x, y, and z. (b) An enlargement of part of this surface showing that the open orbit at 22.5° breaks through at a point (z) nearer to the line AH, i.e., at a point of larger energy gap than the gap (x) broken through by the orbit at 16.1°. The angles φ are marked for these two orbits. For convenience we show φ here as the angle between the surface tangent (perpendicular to $\mathbf{v}$) and the orbit direction (perpendicular to $\mathbf{H}$).

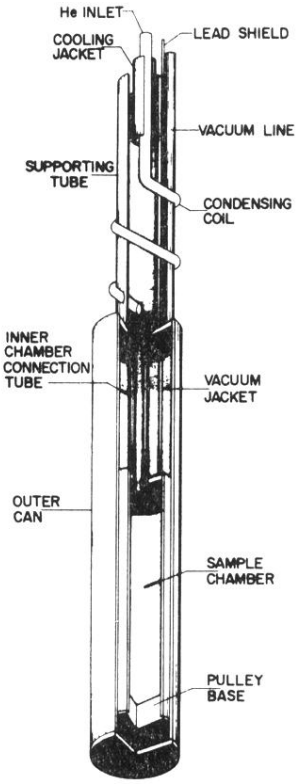

FIG. 4. Inner Dewar system for superconducting solenoid.